Fiber Coupled Cavity Enhanced Thomson Scattering Diagnostic for Use in Electric Propulsion Facilities

IEPC-2019-689

Presented at the 36th International Electric Propulsion Conference
University of Vienna • Vienna, Austria
September 15-20, 2019

Adam J. Friss[1], Tad Wegner[2], and Azer P. Yalin[3]
Colorado State University, Fort Collins, CO, 80523, USA

Pablo Guerrero[4]
California Institute of Technology, Pasadena, CA, 91125, USA

James E. Polk[5] and Lee K. Johnson[6]
Jet Propulsion Laboratory, California Institute of Technology, Pasadena, CA, 91109, USA

We report on the development of a mobile fiber coupled version of the Cavity Enhanced Thomson Scattering (CETS) diagnostic. A summary of CETS progress and development is presented along with a full description of the fiber instrument design. With the use of novel coreless end-capped fiber optics, the high-power CETS interrogation beam was coupled to an in-vacuum optical cavity resulting in intra-cavity powers as high as 3 kW. Collection of Thomson scattering was accomplished with a multi-mode fiber bundle that improved the measurement resolution within the chamber. The instrument was transported to the Jet Propulsion Laboratory where electron temperature and density were measured in the plume of a LaB_6 hollow cathode. The measurement campaign served as a successful proof-of-concept demonstration of the fiber coupled instrument. Several system improvements are identified to enhance the measurement capabilities of the CETS instrument and to help accelerate the adoption of the technique among the EP community.

Nomenclature

AOM	=	Acousto-optic modulator
BaO	=	Barium oxide
CCD	=	Charge coupled device
CETS	=	Cavity-enhanced Thomson scattering
CW	=	Continuous wave
EEDF	=	Electron energy distribution function
EP	=	Electric propulsion
HET	=	Hall effect thruster
HR	=	High-reflectivity
LaB_6	=	Lanthanum hexaboride
LTS	=	Laser Thomson scattering

[1] PhD, Department of Mechanical Engineering, Adam.Friss@colostate.edu.
[2] Graduate Student, Department of Mechanical Engineering, Tad.Wegner@colostate.edu.
[3] Professor, Department of Mechanical Engineering, ayalin@engr.colostate.edu.
[4] Postdoctoral Researcher, Department of Aerospace, pguerrer@caltech.edu
[5] Principal Engineer, Propulsion, Thermal, and Materials Engineering Section, james.e.polk@jpl.nasa.gov
[6] Principal Engineer, Propulsion, Thermal, and Materials Engineering Section, lee.k.johnson@jpl.nasa.gov

n_e	=	Electron density
NIR	=	Near infrared
PDH	=	Pound-Drever-Hall
PMT	=	Photomultiplier tube
PZT	=	Piezo actuator
$\sigma_{Thomson}$	=	Total Thomson scattering cross section

I.Introduction

Improved electron property measurement capabilities in the range of ~10^9 to 10^{12} cm^{-3} are required to advance the study of electric propulsion (EP) devices and would serve to improve the modeling, design, and development of high-power, long-life systems, such as those that will be used for future Mars and Lunar missions[1]. Typically, electron density (n_e) and electron energy distribution function (EEDF) are measured with physical probes (e.g. Langmuir probes), although the use of laser Thomson scattering (LTS) has seen increased use in recent years[2–4]. Physical probes are a crucial tool of the EP and, more generally, plasma physics community. However, due to the requirement of physical contact with the plasma, probes generally result in plasma perturbation and, in some cases, altered plasma device operation. Additionally, the application of probe diagnostics to EP systems can be challenging in regions of high electron temperature, such as within the channel of a Hall effect thruster (HET). While proper design and implementation of a physical probe can reduce measurement error[5], some perturbation will always be present. LTS is an appealing alternative to physical probes due to the non-contact and (generally) non-perturbing nature of the diagnostic, but application of LTS to EP systems is challenging owing to low plasma density[6] (~10^9 – 10^{15} cm^{-3}), a small total scattering cross section[7] ($\sigma_{Thomson}$ = 6.65 x 10^{-29} m^2), and spectral interference from elastic or Rayleigh scattered light positioned at the center of the LTS lineshape[8,9].

Traditional LTS measurements employ nanosecond pulsed laser sources, such as Q-switched Nd:YAG lasers with pulse energies of ~0.1-1 J and repetition rates of ~10-100 Hz, that generate high peak powers of 0.1 to 1 GW but relatively low average powers of ~1-100 W. Due to the low average powers observed with pulsed systems, collection times of many tens of minutes are usually required to resolve the Thomson scattering signal in low-density EP systems of interest. Additionally, the high-peak powers generated with pulsed systems can result in electron temperature and density perturbations via inverse bremsstrahlung[10] and pondermotive interactions[11] respectively. We have developed an alternate method to conventional pulsed LTS, termed cavity enhanced Thomson scattering (CETS), that uses the same spectroscopic approach but relies upon a high-power continuous wave (CW) beam generated within a high-finesse optical cavity as the interrogation light source. The much higher average power observed with the CETS technique results in an increased scattering signal and, due to the much lower peak power, a reduction in the possibility of plasma perturbation. The technique is based upon frequency locking a high-power (~5.3 W) laser source to an optical build-up cavity to generate a ~10-100 kW light source. The CETS diagnostic has been successfully implement and used to measure electron properties in the plume of a hollow cathode[2,12]. Despite the early success of the CETS technique, the application to a variety of EP devices and vacuum facilities necessitated the development of a fully fiber optic coupled version of the instrument. By developing a mobile beamline in conjunction with the rapid installation afforded by fiber coupling the high-power probe beam and Thomson scatter collection, the CETS technique has been further advanced to improve the ease of deployment and to accelerate adoption of the technique by the EP community.

A more detailed explanation of the diagnostic approach and a summary of past work is presented in Section II. The development and implementation of a fiber coupled setup as well as a proof-of-concept demonstration of the instrument to measure electron properties in the plume of a lanthanum hexaboride (LaB_6) hollow cathode is presented in section III. System improvements and future work to aid in the development of a field deployable instrument are presented in section IV. Finally, conclusions are presented in section V.

II.Diagnostic Approach

A. Theory

The free-space CETS diagnostic has been explained in detail in past publications[2,12–18] and, since the theory is the same for both the free-space and fiber version of the instrument, only a brief summary will be presented here. Details of the fiber optic components will be presented in section III. The approach is based upon frequency locking a high-power, narrow-linewidth laser source to a linear high-finesse optical cavity to build-up several kW's of circulating power. The EP device under study is mounted between the cavity mirrors such that the plasma plume and intra-cavity beam overlap. The Thomson scattered light from the intra-cavity beam is gathered via collection optics and directed into a triple monochromator (SPEX), which acts as a wavelength selectable bandpass filter and provides high-suppression of any Rayleigh or stray scatter light that occurs at the laser wavelength. The Thomson signal is dispersed by the triple monochromator onto a near infrared (NIR) photomultiplier tube (PMT) and photon counting operations are performed with an analog multichannel scaler.

The approach takes advantage of a cavity enhanced technique, known as a power-build up cavity, to generate an intense beam of several kW's that serves as the Thomson scattering source. Cavity enhanced techniques offer significant improvements in optical power and therefore scattering signal level in comparison to traditional pulsed LTS systems in which the average power is typically 10-100 W. These improvements come at the cost of added complication, increased instrument and electronics complexity, and restrictions in application environment. While cavity enhanced techniques can be both passive and active, CETS development has focused on active techniques, which tend to result in greater signal enhancement gains. Pound-Drever-Hall[19] (PDH) locking was identified as the most promising of the available active locking techniques owing to a sharp, anti-symmetric error signal and relative insensitivity to laser power fluctuations. The error signal generated with the PDH locking electronics (Toptica, Digilock 110) is used to drive two PID loops that provide laser frequency feedback. A high-speed locking loop drives a double-pass acousto-optic modulator (AOM) that can provide ~80 MHz of extent at a bandwidth of 1-2 MHz. A slow bandwidth loop drives a piezo actuator (PZT) internal to the fiber seed laser that can provide an extent of several GHz but at a limited bandwidth of ~1-3 kHz. The maximum achievable intra-cavity power is limited by the incident laser power, the mirror reflectivity, and the frequency and spatial coupling[20] of the laser to the cavity. NIR CW laser systems with powers ranging from 1-15 W can be acquired, but several kW systems are not yet available. High-finesse mirror sets with reflectiveness R > 0.9999% are commercially available and, with appropriate handling and in-vacuum cavity design, the reflectivity can be maintained for many 100's of hours with minimal degradation. Frequency and spatial coupling are achieved with mode matching optics and a robust locking system. If the laser was perfectly locked to the optical cavity, the coupling factor would approach unity. In such a scenario, the power enhancements scale as 2/(1-R), such that a mirror set with R = 0.99999% would result in a power enhancement of 200,000. In practice, spatial coupling of a well characterized beam is easily achieved with one or more lenses. However, coupling of the beam in the frequency domain requires an ultra-stable optical cavity that may be impractical to implement in an EP vacuum facility. Further, for very high-finesse mirrors, the cavity linewidth can become smaller than the laser linewidth, which ultimately limits the maximum achievable coupling. For example, a 45 cm long optical cavity formed with mirrors of R = 0.99999% results in a cavity linewidth of ~1 kHz. The laser used for this work has a 5 kHz linewidth, so the highest coupling possible with perfect frequency overlap is limited to C = 0.2. Even at relatively low coupling values, the power enhancements afforded by the build-up cavity are substantial and enable Thomson scattering measurements.

B. Summary of Past Work

The CETS diagnostic has progressed from an idea to a fully functional technique capable of sensitive electron temperature and density measurements. Initial development was accomplished with a low-power laser (~20 mW) and a moderate finesse cavity. The low-power diagnostic was designed as a proof-of-concept instrument[13] and test bed to evaluate a variety of methodologies. During development of the instrument, the cavity locking feedback approach evolved and additional components were incorporated into the beam line. Initially feedback was provided by a piezo actuator mounted to the first cavity mirror. Locking studies indicated that the cavity PZT alone was not sufficient to maintain a high-quality lock and led to the fabrication of a custom "cat's eye" double-pass acousto-optic modulator system. The additional feedback provided by the AOM resulted in intra-cavity powers as high as 22 W generated from 3.7 mW of incident power, which corresponds to a power build-up factor of 5900. The low-power setup was coupled to a gas cell and rotational Raman scattering measurements in N_2, O_2, and CO_2 were demonstrated[15,16]. Rotational Raman scattering served a dual purpose, as it was used to calibrate the collection system and provided experimental evidence that a CW laser could be used with an actively locked cavity to enhance the scattering signal and enable measurements that are generally achieved with the use of high-power pulsed laser systems.

After the low-power proof-of-concept demonstration, the diagnostic was reconfigured with the installation of a high-power laser (~5.3 W) and subsequent upgrades of the optical beam line including new optics, a new PDH approach, and an alternate feedback approach. The improvements and higher power light source resulted in intra-cavity powers of several kW's. Additional rotational Raman measurements were performed in laboratory air to confirm the proper operation of the locking setup and to serve as a demonstration of the increased instrument sensitivity afforded by much higher intra-cavity powers[17]. A vacuum chamber compatible version of the diagnostic was developed but, after initial plasma locking results indicated poor performance, a detailed noise study was performed, and a new in-vacuum optical cavity was fabricated[18]. After several system improvements to reduce the system noise and improve the cavity stability successful plasma locking was achieved with intra-cavity powers as high as 11.7 kW generated from 1.64 W of incident laser power, which corresponds to a power build-up factor of 7100.

A BaO hollow cathode measurement campaign was then conducted and served as the first EP application of the CETS instrument. The study was conducted at a variety of cathode conditions and the electron temperature and density were calculated based on the observed Thomson scattering spectra. Data was collected at a fixed discharge current over a variety of propellant flow rates and at a fixed flow rate over a variety of discharge currents. Based on a calculated signal-to-noise of 1100 at an electron density of 3 x 10^{12} cm^{-3} a lower electron density detection limit of ~3 x 10^{9} to ~3 x 10^{10} cm^{-3} for a SNR of 1 to 10 was estimated[2]. The hollow cathode measurement campaign, to the best knowledge of the authors, was the first implementation of a new cavity enhanced variant of laser Thomson scattering for electric propulsion diagnostics. Additionally, an experimental and theoretical study of possible plasma perturbation including heating via inverse Bremsstrahlung, pondermotive density perturbations, and photoionization was performed. Cathode properties were measured at fixed conditions from 4 to 11.7 kW's of intra-cavity power. Both the electron temperature and density remained constant within the error of measurements over the full intra-cavity power range. Theoretical calculations of the minimum fluence to cause a relative temperature perturbation of 1% was performed. Although the calculation was developed for pulsed lasers, by looking at relevant time scales for electron absorption of the CW laser energy a CW fluence of ~5500 J/m^2 was calculated, which is several orders of magnitude below the minimum fluence of 1.19 x 10^8 J/m^2 required for perturbation. A theoretical pondermotive perturbation calculation was performed and indicated that the CETS maximum power level of 11.7 kW would result in negligible perturbation. Finally, photoionization was investigated by comparison to relevant experiments in the literature. While it is possible to ionize neutral propellant via multi photon ionization, based on the intra-cavity laser intensity and the values presented in literature, it is highly unlikely the CETS technique results in any measurable ionization[12].

After the successful completion of the cathode campaign the research direction was shifted from proof-of-concept to the development of a robust, mobile instrument. The free-space instrument worked well, but the small Colorado State University (CSU) vacuum facility used for the cathode campaign was not sufficient to operate high-power cathodes or larger EP devices, such as Hall effect thrusters. Therefore, to make the CETS technique more applicable to a variety of vacuum facilities a fully fiber coupled version of the diagnostic was developed. The instrument was designed around several novel fiber optics including high-power capable single-mode fibers that made use of coreless end-caps and a fiber optic bundle for collection of the Thomson signal. The large foot print of the optical beam line was significantly reduced and re-constructed on a breadboard mounted to a mobile cart that contained the electronics and laser. A second mobile cart to house the SPEX and PMT was also fabricated. As a demonstration of the mobile CETS instrument, a measurement campaign was conducted at the NASA Jet Propulsion Laboratory (JPL) in one of the large vacuum facilities operated by the Electric Propulsion Group. Despite several environmental difficulties, the electron density and temperature in a LaB_6 hollow cathode plume was measured. While the instrument performance was poor compared to the bench-top version of CETS it was successful as a proof-of-concept and yielded a wealth of data that will inform future mobile CETS development. The JPL demonstration, to the best knowledge of the authors, represents the first fully fiber coupled Thomson scattering measurements of an EP device. Fiber collection of Thomson scattering has been used in previous pulsed laser systems[3,21], but the delivery of the high-power scattering beam via a fiber optic cable had not previously been possible.

III.Experimental Setup and Results

After a successful free-space measurement campaign, the next step in CETS development was to reduce the footprint of the instrument and make it mobile to enable testing of EP devices at various large vacuum facilities. All previous work on the CETS diagnostic had been aimed at developing the instrument and demonstrating the technique. Because CETS was built as a proof-of-concept instrument there were few constraints on the size and scale of the beamline and collection system. The initial setup occupied ~80% of a 16 ft. x 5 ft. optical table and an entire 4 ft. tall 19-inch rack mount electronics enclosure. A mobile breadboard configuration has been developed that consists of three distinct modules: optical beamline, collection system, and electronics. The optical beamline is a reduced size re-creation of the original instrument configuration built upon a breadboard on a mobile cart that contains all of the CETS electronics. The high-power CETS beam has been fiber coupled using a special high-power, single-mode fiber optic cable (Thorlabs, P9-1064HE-2) capable of handling up to 15 W of CW power. The collection system consists of the SPEX, PMT, and fiber coupling optics. Because future work will involve a variety of vacuum facilities the collection system was converted from free-space to a multi-mode fiber optic bundle (Thorlabs, BFA105HS02**)** to make the system more flexible and to reduce the setup time required at a new facility. The electronics module consists of the laser, AOM driver, power supplies, computer/DAQ system, photon counter, and Digilock 110. This section discusses the development of the mobile system, fiber optic coupling, and initial hollow cathode measurement results from a test campaign at the Jet Propulsion Laboratory.

A. Novel Fiber Optics

Until recently, coupling of high-power laser beams into single-mode (SM) fibers was not possible due to damage at the face of the fiber caused by extreme laser intensities. The core diameter for a single-mode fiber at 1064 nm is ~ 5 µm resulting in CETS laser intensities (~8 MW/cm^2) well beyond the working damage threshold (~250 kW/cm^2) and even the theoretical damage threshold (~1 MW/cm^2) of existing SM fibers. Past work on high-power fiber coupling, especially for pulsed laser delivery for laser ignition applications[22], has made use of photonic crystal fibers (PCF) which allow for SM operation at core sizes of 30-40 µm. While PCF's would work with the CETS diagnostic they are typically very fragile and expensive, making use in a vacuum chamber problematic. The high-power fiber used to deliver the CETS beam to a vacuum chamber is a SM fiber with special coreless end-caps fusion spliced to each end of the fiber (Fig. 1). The addition of the end-cap allows the beam to be coupled into the fiber at a larger beam diameter, which reduces the beam intensity at the glass-to-air interface where damage typically occurs. Additionally, the fiber is connectorized to make installation easier and repeatable.

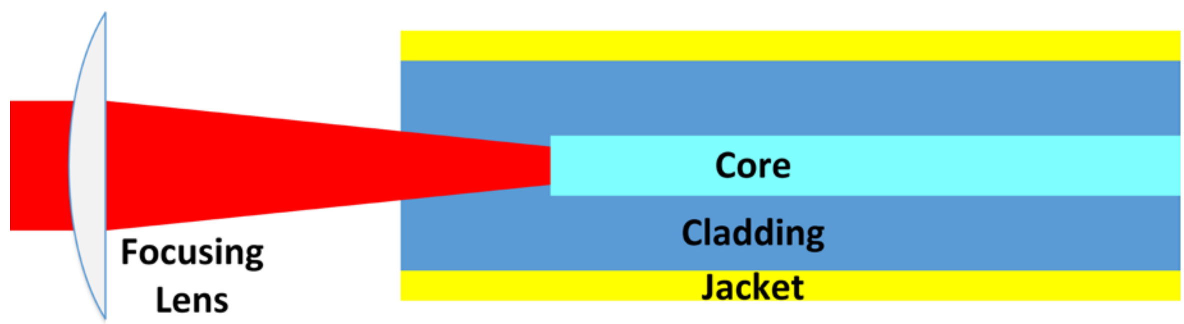

Figure 1. Coreless End-Capped Fiber. *A custom SM fiber optic patch cable was used to couple the high-power CW CETS beam to the in-vacuum optical cavity. A coreless end-cap is used to couple the beam into the fiber at a larger diameter to reduce the intensity at the glass-to-air interface. The core scale has been greatly exaggerated for display.*

In addition to power delivery, fiber optic cables are also used to monitor the cavity transmission and the scattered Thomson signal. The cavity transmission is coupled into a standard multi-mode (MM) patch cable and is used to normalize the scattering data and to monitor the quality of the lock and cavity alignment. Thomson scattered light is collected via optics and imaged onto a linear multi-mode fiber bundle comprised of seven individual fibers. The linear array allows for the collection of a larger region of light within the plasma. Additionally, the use of a linear array allows for greater monochromator throughput as the fibers can be aligned with the entrance slit (Sec. IIID). The cable used for the initial mobile CETS development improved the signal collection compared to the use of a single fiber, but future collection setups would be improved with the use of custom fiber bundles with many more fibers. Custom multi-fiber bundles have been used successfully in past pulsed Thomson work[3].

B. Mobile Cart

The CETS mobile cart beamline (Fig. 2) is similar to the free-space table top layout but the footprint has been reduced in scale and several new fiber optics have been added. A narrow linewidth (<5 kHz) high-power (5.3 W) fiber laser (NP Photonics, RFLSA-5000-3-1064-PM-SA1) serves as the laser source. The output of the laser is coupled to a fixed collimation package and the free-space beam is directed through a Faraday rotator optical isolator to prevent back reflections from coupling back into the laser system. The beam passes through a half wave plate ($\lambda/2$) and polarizing beam splitter (PBS) that sets the polarization direction and can also be used as a variable attenuator during alignment. The PBS, lens, AOM, quarter wave plate ($\lambda/4$), beam block (BB), and concave mirror serve as the double-pass AOM and can be used to frequency shift the beam for PDH locking. The beam exiting the double-pass AOM has been polarization rotated such that it is orthogonal to the input beam and can be picked out of the beamline with the PBS. The beam then passes through an electro-optic modulator (EOM) operating at a modulation frequency of 12.5 MHz to generate laser sidebands that are required for PDH locking. The beam exiting the EOM passes through a beam expander (BE) comprised of two plano-convex lenses to increase the diameter of the beam from ~1.3 mm to ~4.4 mm. The larger diameter beam improves the minimum spot size achievable at the face of the high-power launch fiber (HPSM). A five-axis fiber stage (FS,5A) is used in conjunction with a 15 mm focal length aspheric lens (AS) to couple the high-power beam into the fiber. Fiber coupling as high as 70% has been observed but is difficult to maintain. The mobile diagnostic has been operated successfully with coupling between 50-70% without any apparent fiber damage. The output of the variable attenuator formed with the waveplate and PBS can be coupled into a low-power SM fiber (LPSM) with a 2-axis stage (FS,2A) to be used for rear injection of the SPEX for alignment of the collection optics within the vacuum chamber. One multi-mode fiber, lens, and photodiode (PD) has also been incorporated into the setup to monitor the cavity transmission (LPMM). The reflected cavity signal from the front high-reflectivity cavity mirror is coupled back into the HPSM fiber from the in-vacuum cavity and picked out of the beamline with a thin film beam splitter (BS) and monitored with a fast photodiode. The use of a beam splitter allows for linearly polarized intra-cavity light, which, owing to the polarization dependence of Thomson scattering, boosts the collected signal by a factor of two compared with more traditional PDH setups that use circularly polarized light. A draw back of the BS approach is that a small portion (<3%) of the high-power beam is picked out of the beamline before fiber coupling into a beam dump (BD). The reflected cavity signal suffers from fiber coupling losses and additional noise due to small back reflections at the lens and fiber face but was still used successfully to generate an error signal and to establish a cavity lock.

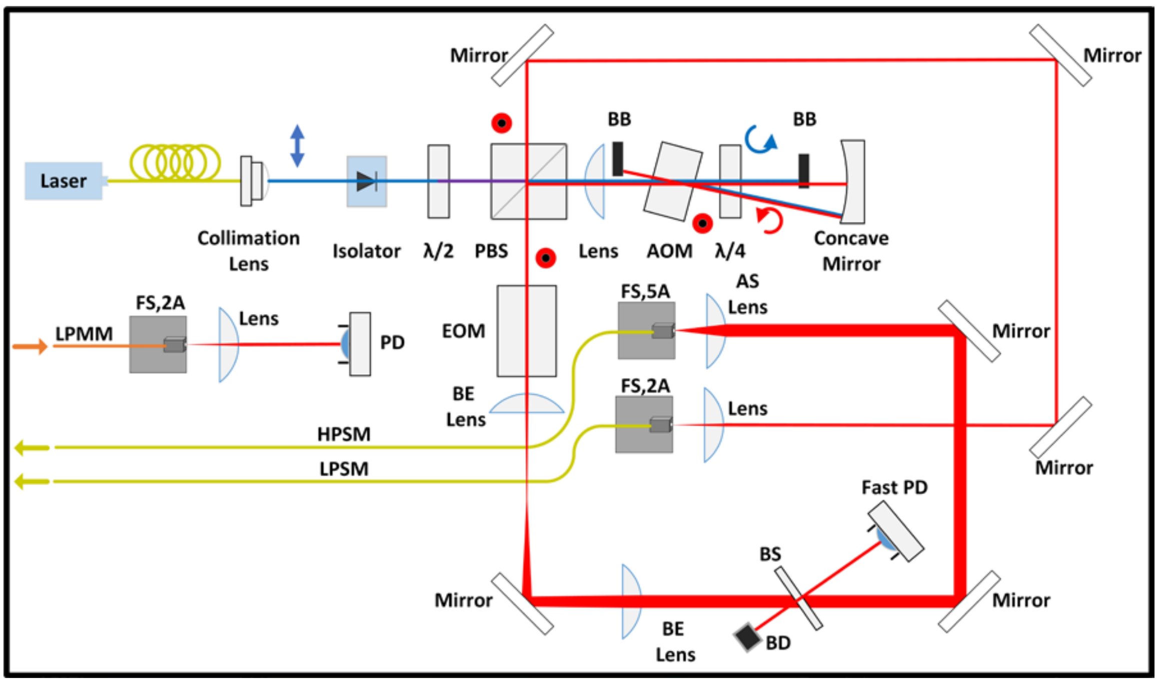

Figure 2. CETS Mobile Cart. *A mobile CETS beamline was constructed on an optical breadboard. Beam polarization states are denoted with red and blue and shown with arrows. All angles have been exaggerated for clarity.*

C. In-Vacuum Optical Cavity

The optical cavity (Fig. 3) has been built from a cage system and installed on a large aluminum frame designed to allow for access to cathodes and Hall effect thrusters up to 40 cm in diameter. To ensure optimal spatial coupling of the high-power beam to the optical cavity, a mode match solution was calculated for the single-mode fiber, commercially available optics, and an optical cavity length of 45 cm. Of the available solutions, the optical path length required between the mode match lens and the first cavity mirror ranged between 1.3 and 2.2 m. Due to the large path length required the cage system extended well beyond the aluminum frame. Additional support was provided to stabilize the cage system and to maintain rigidity. The frame and cage system could accommodate a variety of optical cavity lengths if larger EP devices were tested. The high-power beam is delivered to the in-vacuum cavity via the HPSM fiber cable. A mode matching lens is used to spatially couple the beam to the optical cavity formed with HR1 and HR2. A half-wave plate sets the in-vacuum polarization direction as the SM fiber is not polarization maintaining, so rotation of the polarization is required to ensure proper orientation. The cavity transmission is attenuated using a neutral density optical filter (ND) and coupled into a multi-mode fiber with an off-axis parabolic mirror (OAP) and two-axis fiber stage. The Thomson scattered light is gathered by a multi-mode fiber bundle (7x1 multi-mode fiber with 102 µm core diameter) that is imaged onto the intra-cavity beam with a lens resulting in a measurement region of 900 x 7700 µm. A concave mirror retro-reflector is used to increase the Thomson solid angle of collection.

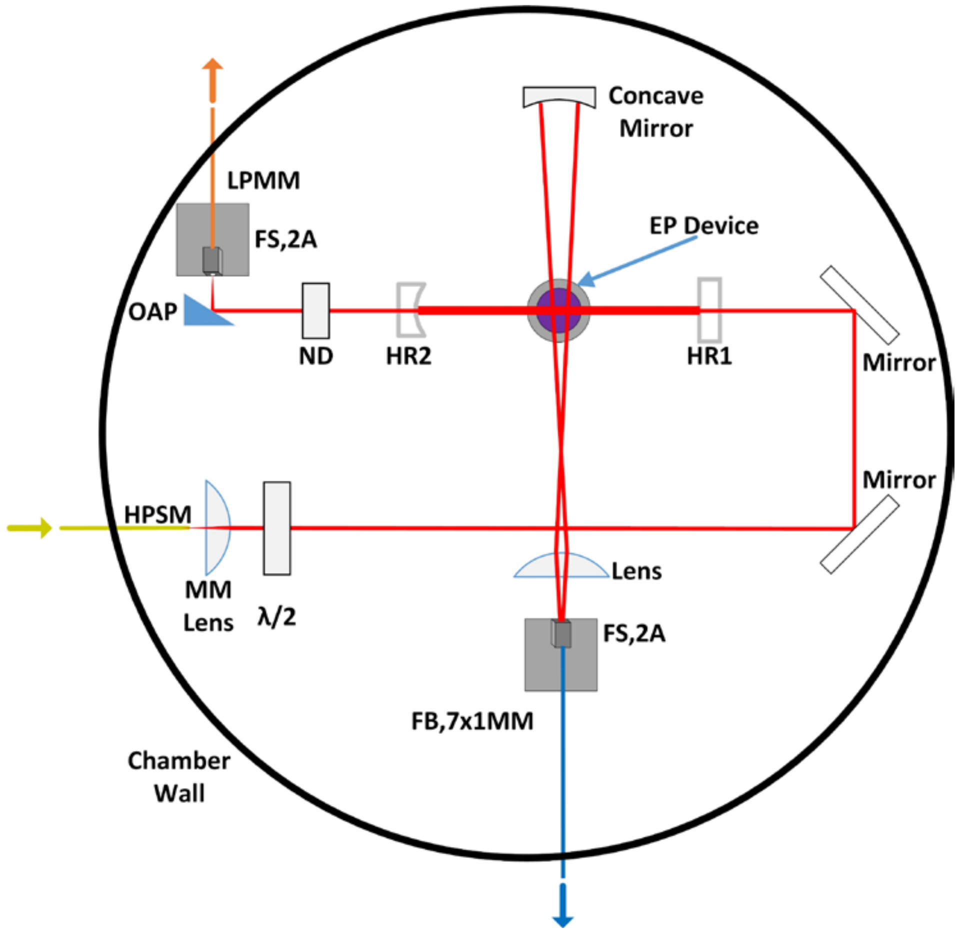

Figure 3. CETS Mobile In-Vacuum Cavity. *The mobile diagnostic uses an aluminum optical cavity equipped with cage optics and fiber connections for rapid installation in vacuum chambers.*

D. Mobile Collection System

The scattered light dispersion and measurement was accomplished with the SPEX, PMT, and multichannel scaler in a similar setup to the bench-top free-space instrument. A second mobile cart was built to mount the SPEX and an optical rail used to set the PMT position with respect to the exit slit (S4). The multi-mode fiber bundle was coupled to the input slit (S1) of the SPEX and imaged to match the NA of the monochromator (Fig. 4). The linear fiber bundle improves the overall light collection and coupling to the SPEX. The PMT was free-space coupled to the SPEX via a collimation lens after the exit slit. The LPSM fiber (from the optical cart) could be coupled to a collimation lens and rear-injected into the SPEX using steering mirrors as an alignment beam (with the PMT removed). The use of this beam allowed for alignment of the internal optics in the SPEX and for positioning of the multi-mode fiber bundle and imaging optic at the entrance slit. The bundle imaging lens position was set based on the magnification requirement but could be translated orthogonal to the beam path with a stage to optimize the coupling. By observing the light exiting the fiber bundle with a CCD and translating the entrance slit optic the signal could be maximized. Two fiber bundle cables were daisy chained due to limitations in the available fiber bundle cable length and vacuum chamber dimension. The coupling of two bundles resulted in reduced throughput. The multi-mode fiber bundle and high-power single-mode fiber were epoxied into a KF vacuum fitting that served as a feedthrough while the multi-mode fiber was passed into the chamber via a compression fitting. Once the in-vacuum cavity optics were installed and aligned the fibers could be removed and the cavity mounting position could be adjusted to access a different plasma region without loss of alignment. Further, the ability to disconnect the fibers enables rapid re-deployment of the diagnostic on multiple chambers in a given lab space with only the need to remove two fiber feedthroughs and to roll the collection and optical cart to the new chamber location.

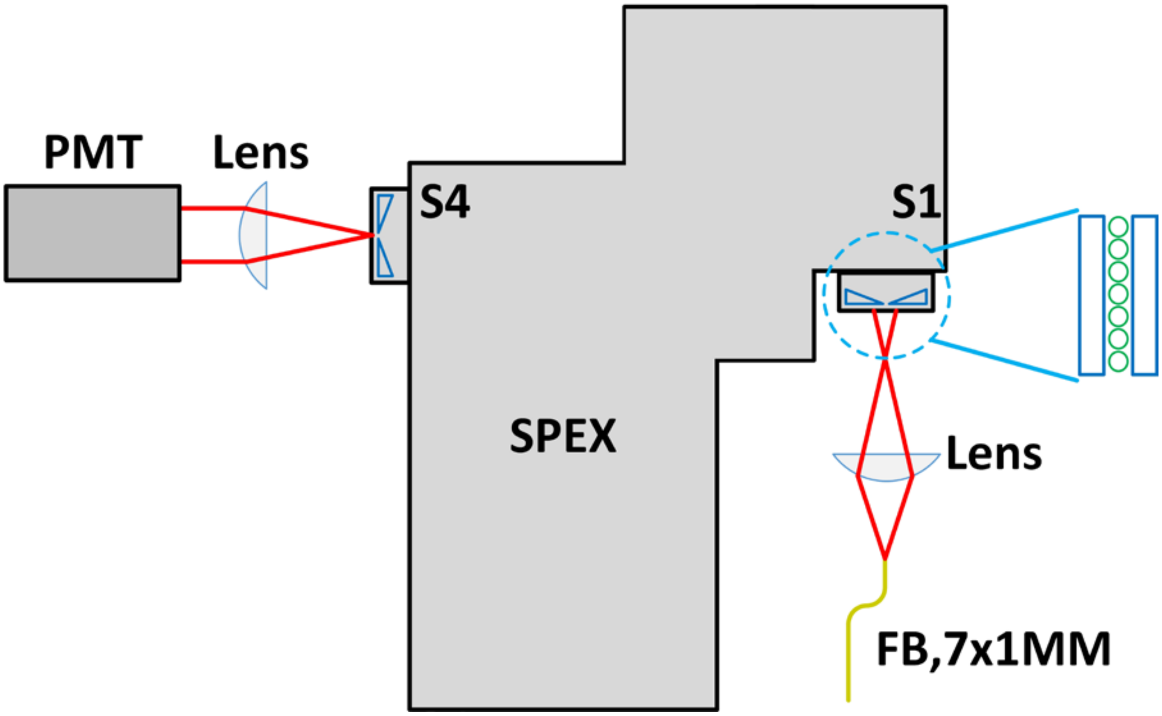

Figure 4. CETS Mobile Collection System. *The Thomson scattered light collected in the vacuum chamber is coupled into the multi-mode fiber bundle. The linear fiber bundle is imaged onto the SPEX entrance slit (S1) such that the fibers are aligned parallel to the slit blades.*

E. Cathode and Vacuum Facility

A lanthanum hexaboride cathode[23] was used as the plasma source for the fiber CETS demonstration. The cathode was installed in the "Big Green" JPL vacuum facility. The chamber has a diameter of 90 inches and is ~18 ft long. A base pressure in the range of 10^{-6} Torr is achieved with three large diffusion pumps. While the chamber is also equipped with cryo-pumps and an LN_2 shroud, only the diffusion pumps were used for the CETS work. A water-cooled copper tube served as the anode and a magnetic trim coil was used to simulate the magnetic field structure present in a Hall effect thruster. The cathode was operated on xenon at a nominal discharge of 20.8 A and flowrate of 14.7 sccm. A 20 mm gap between the cathode and anode provided optical access for the intra-cavity beam and the Thomson collection. The cathode (Fig. 5) was allowed to reach thermal equilibrium before data collection. The CETS in-vacuum optical cavity was mounted about the cathode and foil was used as radiation shielding and to prevent sputter coating of the optics. Despite the large standoff distance and radiation shielding thermal issues were encountered and optical drift was observed over the course of the test campaign.

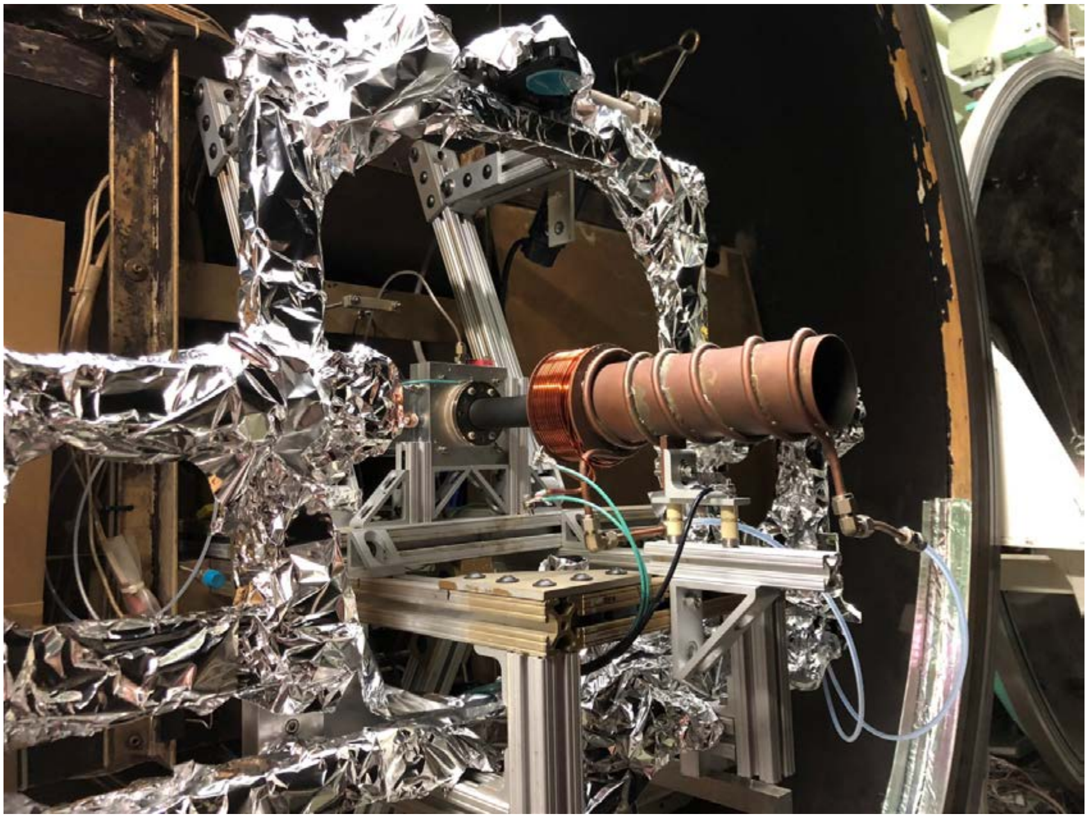

Figure 5. JPL Hollow Cathode Assembly and In-Vacuum Optical Cavity. *A LaB_6 hollow cathode and water-cooled anode with a magnetic trim coil were installed at the JPL vacuum facility. The optical cavity is wrapped in foil to provide some radiation shielding.*

F. Fiber Cavity Locking

Cavity locking using the fiber coupled setup was demonstrated with an intra-cavity power of ~1.5 kW on an optical table at CSU. Despite the lower intra-cavity power, the expected performance of the instrument was similar to the free-space setup due to the much larger collection region within the plasma. Higher power is always more desirable, but some vacuum chambers simply cannot accommodate a free-space setup and therefore require a fiber coupled instrument. After installation in the JPL vacuum facility testing indicated that cavity noise due to vibrations was well beyond the locking bandwidth of the instrument and locking was not possible. Because the JPL chamber is hard coupled to the building and roughing pumps all mechanical noise is transferred directly into the chamber. The in-vacuum cavity was initially hard mounted to the chamber door but, to combat the chamber noise, vibration isolation was added. The cavity was remounted on absorption damping blocks of Sorbothane™ and constrained from moving with respect to the cathode. The addition of vibration isolation reduced the cavity noise to within the locking bandwidth and intra-cavity powers of 1-3 kW's were possible during chamber operation.

Cavity locking could be maintained for many tens of minutes while the vacuum facility was operational, but loss of lock was more frequent than what was observed in the CSU vacuum facility. Additionally, the large temperature fluctuations within the lab space caused frequent misalignment of the high-power fiber stage on the mobile cart. As the lab temperature shifted, the optical breadboard would contract or expand, and the fiber stage would drift. The fiber coupling efficiency was on average 50-55% but would drift as low as 35%. Small adjustments could be made to return the coupling efficiency to the baseline value. The larger and more numerous sources of chamber and environmental noise were the primary cause of the locking issues. As a proof-of-concept, the mobile instrument was sufficient, but future work will require more robust locking electronics, improved vibration damping, and improved long-term beamline stability.

G. Electron Property Measurements

Before the cathode was operated (Fig. 6) a rotational Raman calibration of the collection system was performed. The chamber was pumped down to ~10^{-5} Torr and then backfilled to 50 Torr with pure nitrogen. Based on the Raman data, the collection efficiency was 0.48%. The low efficiency is a consequence of several collection difficulties. It was discovered during the first pump down of the chamber that the multi-mode fiber bundle was creating a large vacuum leak at the feedthrough. In an attempt to reduce or eliminate the leak, the metallic jacket was removed from the fiber bundle and epoxy was injected into the jacket at the feedthrough location. Unfortunately, during the jacket removal, four of the seven fibers were damaged and could not be used for collection of the Thomson signal. Additional losses were incurred by daisy chaining two fiber bundle cables together due to coupling losses and misalignment of the linear bundles with respect to each other. Further losses were due to the imaging of the bundle onto the entrance slit of the SPEX. To match the SPEX NA, the required magnification resulted in a fiber core image of ~300 µm, which over filled the slit width of 100 µm. While the entrance slit could have been enlarged to improve throughput it would have resulted in broadening of the instrument function and would have increased the level of stray light. Despite the low collection efficiency, the larger collection region within the plasma plume and the larger electron density due to higher discharge current were expected to offset the losses.

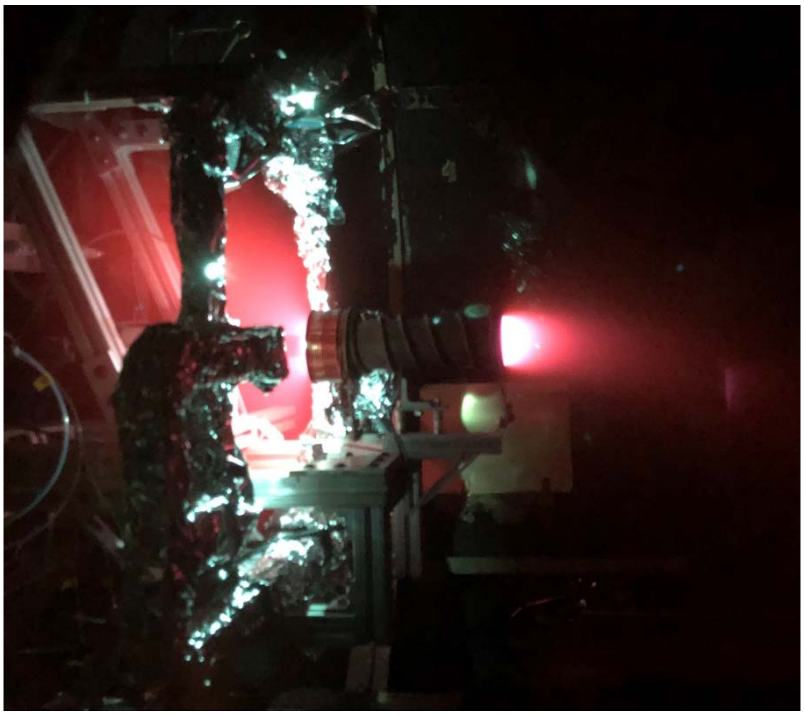

Figure 6. LaB_6 Hollow Cathode Operation. *A LaB_6 hollow cathode was operated at a discharge current of 20.8 A and a flow rate of 14.7 sccm of xenon. A magnetic trim coil was used to simulate the magnetic field conditions in a Hall effect thruster.*

A campaign was conducted to measure electron properties in the plume of the hollow cathode. Over the course of the campaign the quality of the lock degraded, and the intra-cavity power decreased monotonically from 1.4 kW to ~50 W. The decrease in power was likely due to thermal drift of the optical cavity. Additionally, due to the large temperature fluctuations in the lab over the course of the measurement caused by diffusion pump heat rejection and the HVAC system, the high-power SM fiber optic required frequent realignment to ensure proper coupling. Several data sets were acquired, but due to the collection issues and low intra-cavity power the signal-to-noise was poor. Despite the low signal level and large plasma emission background fluctuations, it was still possible to determine the electron density and temperature by performing a non-linear least squares fit of the data. Figure 7 displays the fit of a collected Thomson scattering data set for a discharge current of 20.8 A and a flowrate of 14.7 sccm of xenon. The magnetic trim coil was operated at 15.8 A and the chamber background pressure was 40 µTorr. As determined by the fit, the electron temperature and density was 2.7 eV and 3 x 10^{13} cm^{-3} respectively. The negative data points are a consequence of the subtraction of the Thomson plus plasma emission from the plasma emission background. Due to the large fluctuations of the background emission and the relatively weak Thomson signal, subtraction sometimes produces negative signal levels. Data collection about the laser line center was avoided and the apparent offset of the spectrum to 1065.3 is due to the alignment of the SPEX and multi-mode fiber bundle. Raman measurements were performed to determine the offset but due to resetability issues with the SPEX the line center is left as a free parameter to improve the fitting routine accuracy.

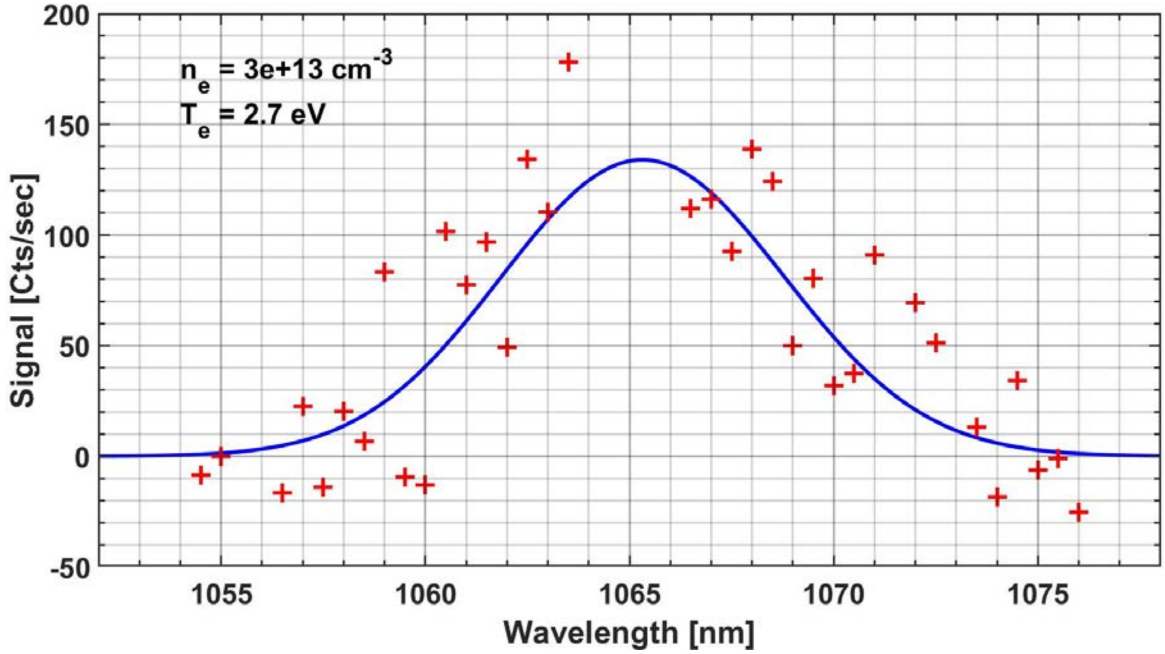

Figure 7. Thomson Scattering Spectrum. *Electron density and temperature were measured in a LaB_6 hollow cathode plasma source operating at 20.8 A, a xenon flowrate of 14.7 sccm, and with a magnetic trim coil. The data (red +) have been fit with a synthetic Thomson spectrum (blue).*

While thermal issues prevented a full sweep of the plasma parameters, the campaign served as a proof-of-concept demonstration and will inform several design changes to ensure future success. The ability to perform fully fiber coupled Thomson scattering measurements makes the CETS diagnostic unique in its ability to be rapidly deployed on a variety of vacuum chambers without the need for optical access. Additionally, because the fibers are connectorized, the cavity can be moved from chamber to chamber with minimal realignment of the optics and cavity. Future work will allow for a more robust instrument with higher intra-cavity powers and improved signal-to-noise. The ultimate goal is a field deployable instrument that can be quickly setup and operated with minimal training or knowledge of fiber alignment or cavity locking.

IV. Next Steps

The CETS technique has great promise and will enable ultra-sensitive measurements of electron properties in low-density plasmas. However, to accelerate the adoption of CETS, work must be done to further improve the performance of the instrument and to make the technique much more robust in the presence of environmental noise. This section focuses on the four areas that would result in significant gains in terms of performance and stability and would further improve the accessibility of the diagnostic to the plasma physics community.

A. In-Vacuum Cavity Design

The length stability requirements to maintain resonance of a high-finesse cavity in the presence of environmental noise are not trivial. The addition of vibration absorbing material enabled the fiber experiments but was not sufficient to achieve the >10 kW intra-cavity power observed with the free-space instrument. Improvements to the optical cavity would result in increased intra-cavity power and would improve the locking tolerance to transient noise that can cause a sudden loss of lock. Significant work has been done in regard to ultra-stable optical cavities[24,25] and vacuum systems specifically for PDH locking. However, these systems are generally intended for laser stabilization to generate ultra-narrow linewidth laser sources and atomic physics experiments. The cavity designs available in literature are generally closed cells made of low expansion materials. Because the CETS technique is intended to be used on EP systems and other plasma sources, the optical cavity must be open. Further, vacuum systems used for ultra-stable cavities do not have the pumping speed required for the operation of most EP devices. The needed application of PDH locking to a high-finesse cavity in a noisy environment is atypical. For use as an EP diagnostic, the CETS technique must be deployable on existing vacuum facilities. Therefore, instead of focusing on ways to reduce the system noise, it would be more beneficial to develop a robust and vibration insensitive optical cavity.

The current in-vacuum cavity is constructed from rigid aluminum bar stock and stainless-steel cage system optomechanics. Because the frame and cage system are exposed to thermal loads warping and distortion are possible. The cage system itself acts as a moment arm and can warp under its own weight. Additionally, vacuum system vibrations can be transferred to the cage system which causes the mirrors to move independently of each other. Vibration isolation should be considered but must take into account the outgassing of the isolation material. An ideal optical cavity would be isolated from chamber vibrations, thermal loads, and would constrain the mirrors with respect to each other. A new cavity design must reduce the movement of the mirrors with respect to each other and should be monolithic so that the mirror mounts are constrained as much as possible. The addition of radiation shielding or thermal stabilization in the form of a cooling or heating loop would further reduce mirror perturbation. Moving to very short optical cavity lengths may also result in improvements as the cavity linewidth increases with a reduction in optical cavity length.

B. Feedback and Locking Electronics

Three ways to provide feedback to the CETS diagnostic have been investigated over the course of development of the technique: a cavity piezo actuator, a laser piezo actuator, and the double-pass AOM system. Scanning via the cavity piezo was limited in bandwidth due to the locking electronics and was limited in performance due to its design. A redesigned cavity piezo could improve the system but would still always be limited in bandwidth by the electronics, the piezo response, preloading force, and the mass of the mirror. However, a cavity PZT could be used to compensate for long term thermal drift of the system and used with an additional PID loop to maintain the locking window with respect to other forms of feedback. It was not possible to implement more than two PID loops in the current system but the addition of a third would improve the lock quality. The laser piezo was sufficient for locking but added significant system noise due to a weak etalon signal. It was possible to lock the system even with the noise and there is little that could be done to rectify the current issue as the PZT is internal to the laser. An alternate approach would be to use a laser system that allows for wavelength modulation via current. If a new laser source was used that could be current modulated, then the bandwidth would improve but etalon effects might still be present. Finally, the double-pass AOM system could be redesigned. The current setup suffers from poor efficiency and limited extent. The efficiency of a beam passed through an AOM is directly related to the beam size and divergence. For a collimated or weakly focused beam, the efficiency can approach 95% on a single pass. However, the modulation bandwidth is a function of beam diameter within the AOM active medium. So, there is an optimum between efficiency and bandwidth. Further, the custom AOM electronics are limited by the range of the commercial voltage-controlled oscillator (VCO) used to drive the RF amplifier. A custom VCO could be designed that would improve the scan extent and improve the locking window for the AOM.

The CETS diagnostic takes advantage of a commercially available digital locking system. While this was an ideal system for CETS development and proof-of-concept it has inherent limitations. The analog to digital conversion introduces measurement error and delay. Analog PDH locking hardware is commercially available and could also be built. While the design of an analog system is not trivial the improvement in locking bandwidth, the addition of more PID loops, and increased speed would be well worth the undertaking. Even building a digital software PDH system using an ultra-fast DAQ card might improve the system as the current unit is FPGA based and was really designed for low- to moderate-finesse cavities in quiet environments.

C. Fiber Optics and Optical Cart

The mobile fiber setup represents the most versatile iteration of the diagnostic. The ability to rapidly deploy an instrument on any chamber without optical access requirements is ideal and an advantage compared with other LTS approaches. While the fiber system was a successful proof-of-concept, many improvements are required before the system can be widely adopted. The fiber setup would benefit from an environment insensitive breadboard and improved fiber optics. The breadboard could be improved by simply adding an insulated housing and a cooling loop for the optomechanics that generate large heat loads. If the temperature of the board could be held constant the fiber alignment drift problem would be eliminated. The high-power fiber worked well but the coupling efficiency must be improved to protect the fiber and to increase the power delivered to the optical cavity. The beam quality before fiber launch could be enhanced if the AOM system is improved as it currently results in a slightly elliptical beam and an increase in M^2. The telescope could also be redesigned to further reduce spherical aberrations. The use of a motorized or piezo actuated five-axis fiber stage would also improve coupling and speed up the setup of the instrument as an automated alignment routine could be used. The high-power SM fiber was epoxied into a feedthrough, which resulted in a vacuum tight seal but restricted the fiber length both inside and outside of the chamber. A compression style feedthrough should be used to allow for fiber movement. Finally, the Thomson collection fiber was poorly suited for a vacuum environment. A custom bundle should be built to improve the collection and light throughput and can be designed to optimize both the plasma collection region and SPEX coupling.

D. Collection System

The collection system efficiency of all iterations of the CETS diagnostic was at best ~ 0.5%. This is due to the poor quantum efficiency of the PMT and the various losses through the triple monochromator. The only way to improve the QE would be to move to visible wavelengths where QE can be as high as 85%. However, narrow-linewidth laser sources are not readily available in visible wavelengths, which would impact the cavity coupling and therefore intra-cavity power. One approach would be to use a titanium sapphire ring laser system where high-powers and relatively narrow-linewidths may be possible. A further benefit of moving to visible wavelengths would be the ability to use an intensified CCD to image the entire Thomson spectrum at once. However, assuming the current laser source or similar sources are used since high-power and narrow-linewidths are readily available, improvements in the collection system efficiency independent of the QE would be beneficial. Several approaches could be considered. Use of a volumetric Bragg grating[3] as a Rayleigh and stray light block would allow the use of a single stage monochromator and would significantly improve collection efficiency. However, use of these gratings can cause beam quality issues and add additional constraints on the collection optics into the monochromator. A novel approach would be to pass the collection beam through low-finesse optical cavities that act as tunable etalons. In this way, the etalon transmission could be scanned to allow for measurement of the Thomson wings while preventing the much stronger elastic light background at the laser wavelength. This approach could also be used to block bright plasma emission lines. Commercial scanning etalons are available, or a custom setup could be designed and fabricated. Use of an etalon system and a single monochromator would result in improved collection efficiency and could be used to isolate plasma emission and stray light.

V. Conclusion

The CETS diagnostic has undergone many iterations and progressed from a low-power proof-of-concept to a high-power fully fiber optic coupled field deployable instrument. The cavity locking feedback approach expanded from a piezo actuator mounted to the first cavity mirror to incorporate a double-pass acousto-optic modulator system that resulted in intra-cavity powers as high as 22 W and a power build-up factor of 5900. Low-power rotational Raman scattering measurements in N_2, O_2, and CO_2 were performed to demonstrate the feasibility of using a CW laser source and optical cavity to detect weak scattering signals. After the scattering demonstration a high-power laser was incorporated into the setup and beam line upgrades were implemented. The improvements and higher power light source resulted in an intra-cavity power of 3.2 kW and build-up factor of 3300. The setup was integrated with a bench-top vacuum chamber and after initial plasma locking results indicated poor performance, a detailed noise study was performed, and a new in-vacuum optical cavity was fabricated. The improved in-vacuum cavity in addition to the installation of new cavity mirrors resulted in successful plasma locking with intra-cavity powers as high as 11.7 kW and a power build-up factor of 7100. A BaO hollow cathode measurement campaign was conducted at a fixed discharge current over a variety of propellant flow rates and at a fixed flow rate over a variety of discharge currents. Based on a calculated signal-to-noise of 1100 at an electron density of 3×10^{12} cm^{-3} a lower electron density detection limit of ~3×10^{9} to ~3×10^{10} cm^{-3} for a SNR of 1 to 10 was estimated but should be experimentally verified. An experimental and theoretical study of possible plasma perturbation including heating via inverse Bremsstrahlung, pondermotive density perturbations, and photoionization was performed, which indicated that it is highly unlikely the CETS technique results in any measurable plasma perturbation. Based on the success of the CETS diagnostic but limited device applicability due to the vacuum chamber and beam line constraints the proof-of-concept setup was redesigned to create a mobile instrument. The mobile setup was only possible due to the use of high-power, single-mode coreless end-capped fiber optics and a fiber optic bundle for collection of the Thomson signal. As a demonstration of the mobile CETS instrument, a measurement campaign was conducted in one of the large vacuum facilities at JPL. Electron properties were measured in the plume of a LaB_6 hollow cathode and served as a proof-of-concept demonstration. Future CETS development will be informed by earlier iterations and improvements in the in-vacuum cavity, locking hardware, fiber optics, and collection system will enable mobile Thomson scattering measurements on a variety of devices. Despite the additional complexity of an optical cavity and frequency locking, the signal improvement and CW nature of the collection provide significant benefit compared with pulsed LTS systems. Finally, the CETS diagnostic should be capable of time resolved studies by repeated triggering of the multichannel scaler by a measured system property, such as the discharge current. In this way, periodic phenomena (e.g. HET breathing mode) can be studied.

Acknowledgments

This work was supported by a NASA Space Technology Research Fellowship (NNX14AL42H) as well as by the NSF/DOE Partnership in Basic Plasma Science and Engineering (DE-SC0010519). The authors would like to acknowledge Ray Swindlehurst and Nowell Niblett for their assistance in running the JPL experimental facility.

References

1. International Space Exploration Coordination Group (ISECG). The Global Exploration Roadmap What is New in The Global Exploration Roadmap? (2018).
2. Friss, A. J. & Yalin, A. P. Cavity-enhanced Thomson scattering measurements of electron density and temperature in a hollow cathode discharge. *Opt Lett* **43**, 5343 (2018).
3. Vincent, B., Tsikata, S., Mazouffre, S., Minea, T. & Fils, J. A compact new incoherent Thomson scattering diagnostic for low-temperature plasma studies. *Plasma Sources Sci. Technol.* (2018).
4. Washeleski, R. L., Meyer, E. J. & King, L. B. Laser Thomson Scattering Measurements of Electron Temperature and Density in the Near-Field Plume of a Hall-Effect Thruster. *Am. Inst. Aeronaut. Astronaut.* (2012). doi:10.2514/6.2012-4118
5. Lobbia, R. B. & Beal, B. E. Recommended Practice for Use of Langmuir Probes in Electric Propulsion Testing. *J. Propuls. Power* **33**, 566–581 (2017).
6. Goebel, D. & Katz, I. *Fundamentals of Electric Propulsion: Ion and Hall Thrusters*. (JPL Space Science and Technology Series, 2008).
7. Hutchinson, I. H. *Principles of Plasma Diagnostics*. (Cambridge University Press, 2005).
8. Bowden, M. D. *et al.* A Thomson scattering diagnostic system for measurement of electron properties of processing plasmas. *Plasma Sources Sci. Technol.* **8**, 203–209 (1999).
9. Muraoka, K. & Kono, A. Laser Thomson scattering for low-temperature plasmas. *J. Phys. D. Appl. Phys.* **44**, 043001 (2011).
10. Carbone, E. a D., Palomares, J. M., Hübner, S., Iordanova, E. & Mullen, J. J. A. M. Van Der. Erratum: revision of the criterion for avoiding electron heating during Laser Aided Plasma Diagnostics (LAPD). *J. Instrum.* **8**, (2013).
11. Shneider, M. N. Ponderomotive perturbations of low density low-temperature plasma under laser Thomson scattering diagnostics. *Phys. Plasmas* **24**, 100701 (2017).
12. Friss, A. J. & Yalin, A. P. Electron Temperature and Density Measurements in a Low- Power Hollow Cathode Discharge by Cavity Enhanced Thomson Scattering. *AIAA Scitech 2019 Forum* (2019). doi:10.2514/6.2019-0192
13. Friss, A. J., Lee, B., Franka, I. & Yalin, A. P. Cavity Enhanced Thomson Scattering for Diagnostics of Weakly Ionized Discharges. *44th AIAA Plasmadynamics Lasers Conf.* (2013). doi:10.2514/6.2013-2763
14. Friss, A., Lee, B., Franka, I. & Yalin, A. P. Towards a Cavity Enhanced Thomson Scattering Diagnostic for Electric Propulsion Research. *33rd Int. Electr. Propuls. Conf.* (2013). doi:10.1098/rsif.2011.0891
15. Friss, A. J., Limbach, C. & Yalin, A. P. Development of a Cavity Enhanced Thomson and Raman Scattering Diagnostic. *54th AIAA Aerosp. Sci. Meet.* (2016). doi:10.2514/6.2016-1698
16. Friss, A. J., Limbach, C. M. & Yalin, A. P. Cavity-enhanced rotational Raman scattering in gases using a 20 mW near-infrared fiber laser. *Opt. Lett.* **41**, (2016).
17. Friss, A. & Yalin, A. Further development of cavity enhanced Thomson scattering for plasma thruster diagnostics. in *53rd AIAA/SAE/ASEE Joint Propulsion Conference* (2017).
18. Friss, A. J. & Yalin, A. P. Status Update: Cavity-Enhanced Thomson Scattering for Electron Measurements in Electric Propulsion Devices. in *35th International Electric Propulsion Conference* (2017).
19. Black, E. D. An introduction to Pound–Drever–Hall laser frequency stabilization. *Am. J. Phys.* **69**, 79 (2001).
20. Kogelnik, H. & Li, T. Laser beams and resonators. *Proc. IEEE* **5**, 1550–1567 (1966).
21. Leblanc, B. P. Thomson scattering density calibration by Rayleigh and rotational Raman scattering on NSTX. *Rev. Sci. Instrum.* **79**, 10E737 (2008).

22. Dumitrache, C., Rath, J. & Yalin, A. P. High Power Spark Delivery System Using Hollow Core Kagome Lattice Fibers. *Materials (Basel).* 5700–5710 (2014). doi:10.3390/ma7085700
23. Goebel, D. M. & Chu, E. High-Current Lanthanum Hexaboride Hollow Cathode for High-Power Hall Thrusters. *J. Propuls. Power* **30**, 35–40 (2014).
24. Alnis, J., Matveev, A., Kolachevsky, N., Udem, T. & Hänsch, T. W. Subhertz linewidth diode lasers by stabilization to vibrationally and thermally compensated ultralow-expansion glass Fabry-Pérot cavities. *Phys. Rev. A - At. Mol. Opt. Phys.* **77**, 053809–1 (2008).
25. Nazarova, T., Riehle, F. & Sterr, U. Vibration-insensitive reference cavity for an ultra-narrow-linewidth laser. *Appl. Phys. B* **83**, 531–536 (2006).